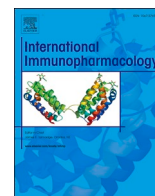




Since January 2020 Elsevier has created a COVID-19 resource centre with free information in English and Mandarin on the novel coronavirus COVID-19. The COVID-19 resource centre is hosted on Elsevier Connect, the company's public news and information website.

Elsevier hereby grants permission to make all its COVID-19-related research that is available on the COVID-19 resource centre - including this research content - immediately available in PubMed Central and other publicly funded repositories, such as the WHO COVID database with rights for unrestricted research re-use and analyses in any form or by any means with acknowledgement of the original source. These permissions are granted for free by Elsevier for as long as the COVID-19 resource centre remains active.



Pexidartinib (PLX3397) through restoring hippocampal synaptic plasticity ameliorates social isolation-induced mood disorders

Laifa Wang^{a,b,1}, Xueqin Wang^{a,b,1}, Ling Deng^{a,b}, Hui Zhang^{a,b}, Binsheng He^{a,b}, Wenyu Cao^{c,*}, Yanhui Cui^{a,d,*}

^a Neuroscience and Behavioral Research Center, Academician Workstation, Changsha Medical University, Changsha, Hunan 410219, China

^b Hunan Key Laboratory of the Research and Development of Novel Pharmaceutical Preparations, Changsha Medical University, Changsha, Hunan 410219, China

^c Clinical Anatomy & Reproductive Medicine Application Institute, Hengyang Medical School, University of South China, Hengyang, Hunan 421001, China

^d Center of Respiratory Medicine, Xiangya Hospital, Central South University, Changsha, Hunan 410008, China

ARTICLE INFO

Keywords:

Social isolation
Pexidartinib
Microglia
Neuroprotection

ABSTRACT

Social behavior is essential for the well-being and survival of individuals. However, social isolation is a serious public health issue, especially during the COVID-19 pandemic, affecting a significant number of people worldwide, and can lead to serious psychological crises. Microglia, innate immune cells in the brain, are strongly implicated in the development of psychiatry. Although many microglial inhibitors have been used to treat depression, there is no literature report on pexidartinib (PLX3397) and social isolation. Herein, we adopted PLX3397 to investigate the role of microglia in the modulation of social isolation. Our results found that social isolation during adolescence caused depressive-like, but not anxiety-like behavior in mice in adulthood, with enhanced expression of the microglial marker Iba1 in the hippocampus. In addition, treatment with PLX3397 reduced the expression of the microglial marker Iba1, decreased the mRNA expression of IL-1 β , increased the mRNA expression of Arg1, elevated the protein levels of DCX and GluR1 and restored the dendritic spine branches and density, ultimately mitigating depressive-like behavior in mice. These findings suggest that inhibition of microglia in the hippocampus could ameliorate mood disorders in mice, providing a new perspective for the treatment of psychiatric disorders such as depression.

1. Introduction

Appropriate social behaviors are essential for the well-being and survival of individuals [1]. However, social isolation, defined as the objective absence of social contact and reduced social network size [2], is a serious public health issue affecting a significant number of people worldwide. In recent years, the coronavirus disease 2019 (COVID-19) crisis has posed a pervasive threat to the overall health of all populations. In addition to the disease itself [3], accumulating evidence has demonstrated that the adoption of segregation during the COVID-19 pandemic caused social isolation, which is also associated with dementia and mental health conditions [4–7]. Although interventions addressing social isolation have been studied, their effectiveness is limited [8]. Therefore, further exploration of the mechanisms underlying social isolation might be beneficial for the optimized treatment of

disorders associated with social deficits.

Neuroinflammation is suggested to be a mechanism implicated in behavioral disorders, such as depression [9–11]. Microglia, key cells involved in neuroinflammation, play critical roles in development and homeostasis, as well as in injury and diseases [12–14]. Numerous studies have shown that microglia can promote neurite formation, synaptogenesis, and myelination and regulate synaptic pruning [15]. In the resting state, microglia have small cell bodies and are highly ramified, and their processes are highly dynamic, which facilitates the monitoring and stabilization of homeostasis in the brain [16]. During disease, injury, or stress, microglia are activated and secrete neurotoxic proinflammatory cytokines, which further eliminate synapses and suppress hippocampal neurogenesis [17–19]. In fact, after treatment with microglia inhibitors, such as minocycline, chronically stressed animals showed improved cognitive behavior and alleviated depression-like

* Corresponding authors at: Clinical Anatomy & Reproductive Medicine Application Institute, Hengyang Medical School, University of South China, Hengyang, 421001 Hunan, China. Neuroscience and Behavioral Research Center, Academician Workstation, Changsha Medical University, Changsha, Hunan 410219, China.

E-mail addresses: marksman0@163.com (W. Cao), cuiyanhui0110@163.com (Y. Cui).

¹ These authors contributed equally to this work.

<https://doi.org/10.1016/j.intimp.2022.109436>

Received 26 August 2022; Received in revised form 1 November 2022; Accepted 4 November 2022

Available online 14 November 2022

1567-5769/© 2022 Elsevier B.V. All rights reserved.

behavior, which might be due to normalized microglial function [20–22]. Consistently, recent studies showed that minocycline could normalize the depression-like behavior induced by chronic social isolation in mice [23,24]. However, minocycline is suggested to function as an antibiotic, which might confound its effect [25,26]. Thus, using more specific methods to delete microglia might provide more information to address this issue.

PLX3397, a colony-stimulating factor 1 receptor (CSF1R) inhibitor, had the strongest inhibitory effect on microglia [27]. It has been reported that continuous administration of PLX3397 can clear microglia in the brain, but microglia will gradually recover and regenerate when drug administration is stopped [28]. Therefore, in this study, we aimed to illustrate the role of the deletion of microglia by PLX3397 in socially isolated mice. Our results demonstrated that social isolation could induce depressive-like behavior in mice in adulthood, coupled with activation of microglia in the hippocampus. Importantly, the deletion of microglia by PLX3397 effectively attenuated depressive-like behavior, which might be due to the rebalance of pro-/anti-inflammatory cytokines, with modulation of the GluR1 subunits of the glutamate receptor, thus boosting neurogenesis and enhancing synaptic plasticity.

2. Materials and methods

2.1. Animals

Three- to four-week-old male C57BL/6 mice purchased from Hunan SJA Laboratory Animal Corporation Limited were divided into group-housed (GH) and socially isolated (SI) groups. Group-housed (GH) mice were housed at 7 animals (460 × 300 × 160 mm) per cage. Socially isolated (SI) mice were raised one per cage (290 × 178 × 160 mm) for 9 weeks. The mice were kept in a quiet, clean and well-ventilated room with a room temperature of 22–24 °C, a relative humidity of 55%–60%, and a circadian rhythm of 12 h. The mice had free access to food and water. The behavioral tests were performed in the 9th week.

2.2. Drug

PLX3397 was purchased from ShangHai Superlan Chemical Technique Centre and mixed into the rodent chow supplied at a dosage of 290 mg/kg. Socially isolated mice were divided into three groups: SI group (treated with normal chow), PLX3397 1w (treated with PLX3397 chow for one week, which was then replaced with normal chow for a week), and PLX3397 2w (treated with PLX3397 chow for two weeks). The PLX3397 chow was administered from the 7th week.

2.3. Behavioral procedure

2.3.1. Open field test (OFT)

The open field test was performed to assess motor ability and anxiety-like behaviour [29]. In this experiment, a 40 cm × 40 cm × 40 cm device was used. The bottom of the open field was evenly divided into 25 grids, and the central 9 grids were defined as the central region. Before the experiment, the mice were familiarized with the environment for 1 h. At the beginning of the experiment, mice were placed into the center of the open field, and the total distance the mice traveled in the open field and the percentage of time spent in the central area within 5 min were recorded by a Smart 3.0 (Shenzhen Rayward Life Technology). The arena was cleaned with 75% ethanol between trials to avoid residual odors. The observers were blinded to the experimental conditions.

2.3.2. Forced swimming test (FST)

The forced swimming was used to detect desperate behavior in mice [30]. During the experiment, mice were placed in a transparent plastic bucket of 10 cm (diameter) × 30 cm (height), which was filled with water at a temperature of 23°C ± 2 °C and a height of 10 cm. The percentage of time mice spent immobile within 6 min was recorded by a Smart 3.0. Immobility was characterized as no active movements. Each animal was dried with a towel and returned to their home cage after the test.

2.3.3. Tail suspension test (TST)

The principle of the tail suspension test is that a mouse suspended from its tail is unable to escape from the impasse and then shows desperate behaviour [31]. During the experiment, the tail of each mouse was fixed on a suspension box (height 40 cm, width 30 cm) with medical tape, and the percentage of time the mice spent immobile within 6 min was analyzed by a Smart 3.0. Immobility was defined as when the mouse hung passively and completely motionless.

2.4. Immunohistochemistry (IHC)

The mice were euthanized with 1% pentobarbital sodium for immunohistochemistry after behavior testing. The mice were transcardially perfused with 0.9% saline and 4% paraformaldehyde (PF) in turn. The brain was completely removed, immersed in 4% PF overnight, and then transferred to 15% and 30% sucrose solution for dehydration. Finally, the brains were coronally sectioned on a cryostat at 30 μm thickness, and sections were stored in 0.01 M PBS and moved to 3% hydrogen peroxide solution for 15 min to remove endogenous peroxidase. Then, the sections were blocked with 5% BSA containing 0.2% Triton X-100 at room temperature for 1 h. Next, the sections were incubated with primary antibody (anti-Iba1, 1:2000) overnight. The next day, sections were incubated with secondary antibody (biotinylated goat anti-rabbit IgG secondary antibody, 1:200) at room temperature for 2 h after washing and then incubated with the third antibody (VECTASTAIN® ABC HRP Kit) at room temperature for 1 h after washing. Finally, the sections were stained with a DAB kit, mounted on slides and dried at room temperature. Finally, the slices were coverslipped with neutral balsam medium (Sinopharm, China) after dehydration using graded ethanol and vitrification by dimethylbenzene. Images were acquired using a microscope (Leica) with identical exposure settings. Data were acquired from 3 mice and at least 3 brain slices from each mouse. The data were averaged to produce a single value per subject.

2.5. Reverse transcription real-time quantitative PCR (RT-qPCR)

Mice were anesthetized with 1% pentobarbital sodium, and the hippocampus was isolated and frozen at – 80 °C. RNA was extracted using TRIzol® (Invitrogen, USA) following the manufacturer's instructions. The cDNA was generated using the High-Capacity cDNA Reverse Transcription Kit (Vazyme, R223-01) and processed for real-time PCR quantification in the QuantStudio 3 Real Time PCR System (Applied Biosystems, USA). The primer sequences are as follows:

Genes	Forward primer	Reverse primer
IL-1 β	TGCCACCTTTGACAGTGATG	AAGGTCCACGGGAAAGACAC
Arg1	CTCCAAGCCAAAGTCCTTAGAG	AGGAGCTGTCATTAGGGACATC
BDNF	CAGCCTACACCGCTAGGAAG	GTCGCCCTTAAAAGCGTCT
IGF2	CTTCTCTCCGATCCTCTG	CAACATCGACTTCCCCACTG
GAPDH	GGTGAAGGTCGGTGTGAACG	CTCGCTCCTGGAAGATGGTG

2.6. Western blot (WB)

Mice were euthanized with 1% pentobarbital sodium, brains were quickly removed, and the hippocampus was isolated. Then, hippocampal tissue protein was extracted as previously described [32]. The tissue was homogenized in a mixture with tissue protein extraction and protease inhibitor (Thermo Fisher Scientific). The supernatant was collected after centrifugation at 4 °C for 20 min at 12000 rpm and denatured for 8 min. Equal amounts of protein were separated by a 9% SDS-PAGE gel at 110 V for 2 h and transferred to a 0.45 μ m nitrocellulose membrane. Then, the membranes were blocked with 5% skim milk at room temperature for 1 h, followed by incubation with primary antibody overnight at 4 °C. The primary antibodies included anti-NR1 antibody (1:1000, Rb, Abcam), anti-NR2A antibody (1:500, Rb, Abcam), anti-NR2B antibody (1:500, Ms, Abcam), anti-DCX antibody (1:1000, Rb, Abcam), anti-Iba1 antibody (1:1000, Rb, Abcam), anti-PSD95 antibody (1:1000, Ms, Abcam), anti-SYN antibody (1:8000, Rb, Abcam), anti-GluR1 antibody (1:1000, Rb, Abcam), anti-GluR2 antibody (1:1000, Rb, Proteintech), and anti-iNOS antibody (1:1000, Rb, Proteintech). On the second day, the membrane was incubated with secondary antibody (HRP-labeled sheep anti-rabbit secondary antibody, 1:2000) for 2 h and was then developed by an ECL imaging system. The densitometric values of bands were measured by ImageJ software (NIH).

2.7. Golgi staining

Golgi staining was performed according to the experimental methods provided by the FD Rapid Golgistain Kit (FD NeuroTechnologies) [30,33]. Mice were anesthetized with sevoflurane, and their brains were removed quickly. The brains were gently dipped in distilled water, and residual blood was washed with plastic tweezers, after which the brain tissue was immersed in the supernatant of a mixture of A and B prepared in advance at 24 h (stored at room temperature and protected from light). The brain tissue was soaked for two weeks in a new A and B mixture after 24 h. Next, the brain tissue was immersed in solution C and soaked for another 7 days in a new solution C after 24 h. Then, 100 μ m slices were dried at room temperature in the dark. A few drops of 30% sucrose solution were added to the slide with a pipettor, and sucrose solution allowed the brain slice to adhere to the slide. The section was then transferred with a glass specimen retriever onto a slide, and a fine paint brush was used to adjust the position of the section so that it was flat and oriented on the slide. A lens cleaning paper (GE Healthcare, Chicago, IL, USA, catalog number: 10149470) was used to cover the section to protect it from damage or any movement. A piece of filter paper was used to absorb the excess solution. Gentle pressure was applied on the filter paper with fingers so that no air bubbles or solution were present between the section and the slide. Then, the lens cleaning tissue was carefully removed. The sections were mounted on slides in racks and kept in a dark room to dry overnight. Finally, the cells were stained with solution D and solution E. Images were acquired using a microscope (Leica) and analyzed by Fiji. The length of dendrites and the number of dendritic branches were analyzed by Sholl analysis.

2.8. Sholl analysis

Sholl analysis was performed as described in a previous study [34–36]. We scanned images of all slices by a Panoramic 250 FLASH II digital slide scanner (3DHISTECH, Budapest, Hungary) and acquired the images with a 40 \times objective lens by CaseViewer 2.4.0. Then, the images were imported into and processed using Fiji. First, we converted each image to an 8-bit image and autosubtracted the background and then randomly selected a representative sample from each image for Sholl analysis. Three mice were analyzed in each group (5 cells per animal for microglia), with a total of 15 cells.

2.9. Statistical analysis

GraphPad Prism 8.0 software (GraphPad Software, Inc., La Jolla, CA, USA) was used for statistical analysis of the experimental data, and the experimental results are presented as the mean \pm standard error (mean \pm SEM). Student's *t* test was used to compare two groups, and one- or two-way ANOVA was used for comparisons of three or more groups followed by Tukey's multiple comparisons test. $p < 0.05$ was considered a statistically significant difference.

3. Results

3.1. SI induced depression-like behavior accompanied by the activation of hippocampal microglia

We performed several behavioral tests to explore behavior in mice (Fig. 1A). In the OFT, we found that the percentage of time spent in the center of the open field was not different between the two groups ($t = 0.4414$, $p = 0.6657$; Fig. 1B). The total distance traveled by SI mice was significantly increased compared with that traveled by GH mice ($t = 6.269$, $p < 0.0001$; Fig. 1C), suggesting that SI did not induce anxiety-like behavior but increased motor ability in mice. Then, the FST and TST demonstrated that the percent immobility time of SI mice was significantly elevated compared to that of GH mice in both the FST ($t = 3.745$, $p = 0.0022$; Fig. 1D) and the TST ($t = 6.318$, $p < 0.0001$; Fig. 1E). Taken together, these results indicated that SI leads to depressive-like but not anxiety-like behavior in mice. Next, we detected the expression of Iba1 in the hippocampi of mice by IHC, and the results showed that the average optical density was markedly upregulated in the CA1 ($t = 4.053$, $p = 0.0154$; Fig. 2B), DG ($t = 11.68$, $p = 0.0003$; Fig. 2C) and CA3 ($t = 4.250$, $p = 0.0132$; Fig. 2D) regions of the hippocampus in the SI group. These findings suggested that SI could induce depression-like behavior along with the activation of microglia.

3.2. PLX3397 treatment ameliorated depression-like behavior induced by SI

To investigate the effects of PLX3397 on the behavior of mice, we treated mice with PLX3397 from the 7th week for one or two weeks to observe its effects on behavior. One-way ANOVA showed that there were no differences in the percentage of time spent in the center in the OFT among the four groups ($F(3, 24) = 0.5073$, $p = 0.6809$; Fig. 3B).

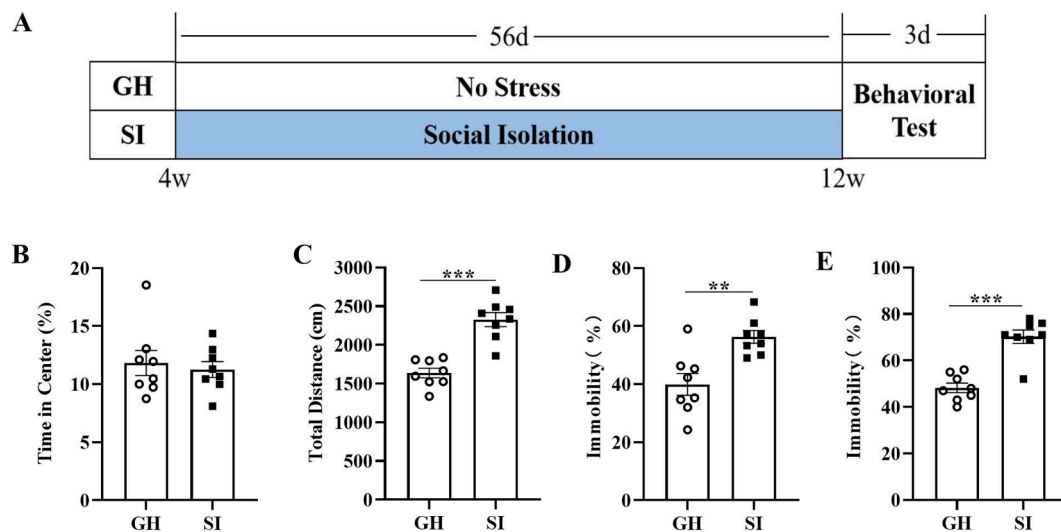


Fig. 1. SI induces the depressive-like but not anxiety-like behavior in mice. (A) Schematic of the experimental procedure. Percentage of time spend in the central area (B) and total distance (C) between two groups in the OFT. Percentage of time spent immobile in the FST (D) and TST (E). ** $p < 0.01$, *** $p < 0.001$ vs. GH group, $n = 8$ /group.

That total distance of the SI group ($t = 4.333$, $p = 0.0256$; Fig. 3C) was significantly increased compared with the GH group, and the total distances of the PLX3397 1w ($t = 8.865$, $p < 0.0001$; Fig. 3C) and PLX3397 2w ($t = 6.004$, $p = 0.0015$; Fig. 3C) groups were significantly increased compared with the SI group, which revealed that PLX3397 treatment could increase the motor capacity of mice. We also found that SI mice showed significantly increased immobility time compared with the GH group in the FST ($t = 5.356$, $p = 0.0047$; Fig. 3D) and the TST ($t = 5.089$, $p = 0.0073$; Fig. 3E). Furthermore, the PLX3397 1w ($t = 7.643$, $p < 0.0001$ for FST; $t = 5.163$, $p = 0.0065$ for TST; Fig. 3D and E) and 2w ($t = 8.655$, $p < 0.0001$ for FST; $t = 6.559$, $p = 0.0006$ for TST; Fig. 3D and E) groups exhibited significantly reduced immobility time. Taken together, these results indicated that PLX3397 treatment could mitigate depressive-like induced by SI.

3.3. PLX3397 treatment ameliorated microglial activation and induced morphological alterations in the hippocampus

We detected the expression of Iba1 in the hippocampus of mice by IHC, and the results showed that compared with those in the SI group, the average optical densities were increased in the CA1 ($t = 5.714$, $p = 0.0158$; Fig. 4B), CA3 ($t = 10.61$, $p = 0.0003$; Fig. 4C) and DG ($t = 5.427$, $p = 0.0207$; Fig. 4D) regions of the hippocampus in the GH group. Conversely, the densities in the SI + PLX3397 1w (CA1: $t = 5.548$, $p = 0.0185$, CA3: $t = 9.576$, $p = 0.0006$, DG: $t = 8.014$, $p = 0.0021$; Fig. 4B-D) and SI + PLX3397 2w (CA1: $t = 6.621$, $p = 0.0069$, CA3: $t = 11.16$, $p = 0.0002$, DG: $t = 8.688$, $p = 0.0012$; Fig. 4B-D) groups were significantly decreased. In addition, we explored the morphological changes in microglia by Sholl analysis. Statistical analyses of complexity showed that SI induced amoeboid microglia, such as shorter and thicker processes, enlarged cell bodies, and less complex branches, while the PLX3397 1w group showed evidence of restoration. In addition, we also observed changes in Iba1 by WB, as indicated by our findings that the protein levels of Iba1 were upregulated in socially isolated mice ($t = 9.720$, $p < 0.0001$; Fig. 5C), while the expression levels were reduced in SI + PLX3397 1w ($t = 15.01$, $p < 0.0001$; Fig. 5C) and 2w ($t = 14.79$, $p <$

0.0001 ; Fig. 5C) mice. In conclusion, PLX3397 treatment for 1 w or 2 w inhibited the activation of microglia.

3.4. PLX3397 treatment ameliorated SI-induced behavioral disorders by enhancing neurogenesis and synaptic plasticity

Based on previous results, to clarify the role of PLX3397 in social isolation, we detected changes in cytokine factors in four different groups. We found that the mRNA levels of IL-1 β were increased in the SI group ($t = 4.066$, $p = 0.0427$; Fig. 6A) compared with the GH group, and PLX3397 treatment reversed this increase (1w: $t = 4.872$, $p = 0.0126$; 2w: $t = 4.639$, $p = 0.0181$; Fig. 6A), while the mRNA levels of Arg1 ($t = 5.395$, $p = 0.0055$; Fig. 6B) in SI were decreased, while PLX3397 treatment could reverse this effect, including Arg1 (1w: $t = 5.527$, $p = 0.0045$; 2w: $t = 4.654$, $p = 0.0176$; Fig. 6B), but there were no changes in BDNF (Fig. 6C) and IGF2 (Fig. 6D) in the four different groups, although BDNF had a downward trend compared with the GH group ($t = 3.936$, $p = 0.0516$; Fig. 6C). In addition, the protein level of iNOS in socially isolated mice was obviously increased ($t = 12.09$, $p < 0.0001$; Fig. 6E and F), and PLX3397 reduced its expression (1w: $t = 13.82$, $p < 0.0001$; 2w: $t = 14.20$, $p < 0.0001$; Fig. 6E and F) These findings suggest that PLX3397 treatment could maintain the balance in pro-/anti-inflammatory cytokines.

Previous studies have found that neurogenesis and neuroplasticity are important in the pathogenesis of mental illness. Therefore, we assessed the expression of DCX by WB. PLX3397 treatment reversed the decrease in DCX induced by SI (1w: $t = 5.674$, $p = 0.0081$; 2w: $t = 7.742$, $p = 0.0007$; Fig. 6E and 6G), and we also observed changes in synaptic-related genes, such as NMDAR (NR2A and NR2B), AMPAR (GluR1, GluR2), the presynaptic protein SYP, and the postsynaptic protein PSD95 in the hippocampus by WB. Our results showed that SI significantly decreased the expression of GluR1 in the hippocampus ($t = 5.038$, $p = 0.0034$; Fig. 6H and 6I), and PLX3397 treatment reversed this decrease (1w: $t = 5.050$, $p = 0.0033$; 2w: $t = 5.984$, $p = 0.0003$; Fig. 6H and 6I). However, no differences were observed in NR2A, NR2B, GluR2, PSD95 or SYP (Fig. 6H and 6I). To further explore the effects of PLX3397

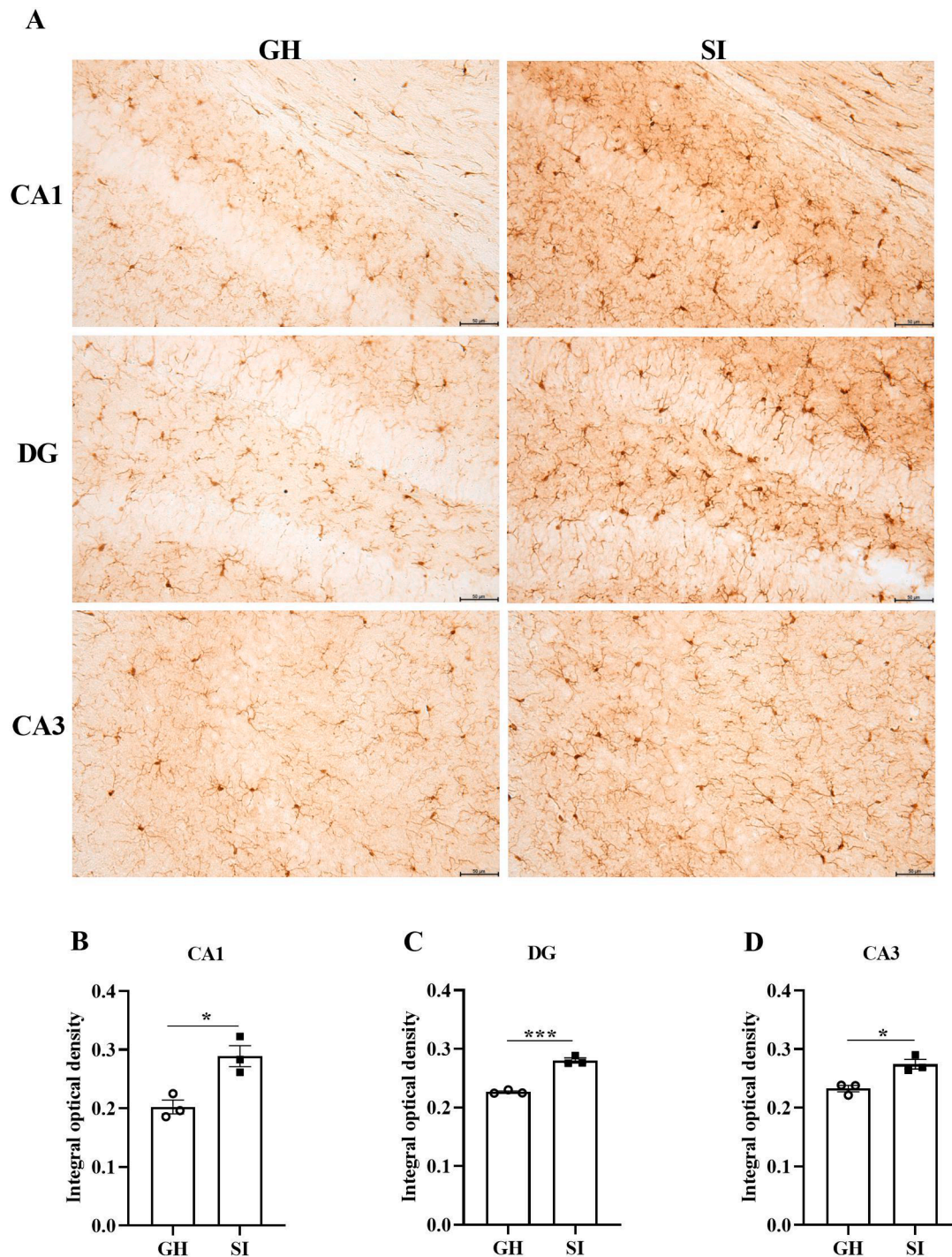


Fig. 2. SI induces the activation of microglia in the hippocampus. (A) Representative immunohistochemical images of Iba1 are presented for the hippocampal CA1, CA3 and DG areas in two groups. The statistical results of Iba1 expression in the CA1 (B), DG (C) and CA3 (D) areas. * $p < 0.05$, *** $p < 0.001$ vs. SI group, $n = 3/\text{group}$, scale bar = 50 μm .

treatment on synaptic plasticity, we detected dendrite length, number of dendrite branches and density of dendrite spines by Sholl analysis. Our results demonstrated that SI induced a decrease in dendrite length and reduced the number of dendrite branches ($F(3, 612) = 103.1$, $p < 0.0001$; Fig. 7A and 7D) and the density of dendrite spines ($t = 6.464$, $p = 0.0010$; Fig. 7B and 7C), and the PLX3397 1w and 2w groups could restore these parameters (1w: $t = 5.897$, $p = 0.0025$; 2w: $t = 6.397$, $p = 0.0011$; Fig. 6H and 6I). Taken together, our results showed that PLX3397 could improve mood disorder by relieving neuroinflammation, boosting neurogenesis and restoring synaptic plasticity.

4. Discussion

In this study, we demonstrated that socially isolated mice exhibited depressive-like behavior, with increased expression of Iba1 in the hippocampus. Furthermore, deleting microglia with PLX3397 normalized the phagocytosis and release of pro-/anti-inflammatory microglia and alleviated depressive-like behavior in mice.

Social isolation acts as a stressor and can cause changes in social behavior in both animals and humans and has been considered a major risk factor for morbidity and mortality in humans in recent years

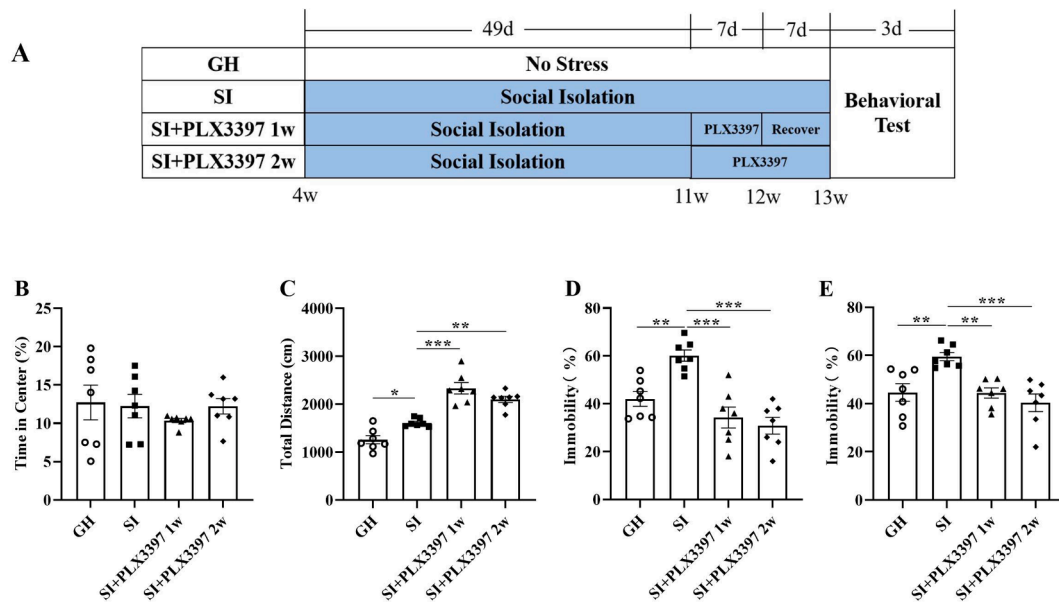


Fig. 3. PLX3397 treatment ameliorates SI-induced behavior disorder. (A) Schematic diagram of the experimental process. Percentage of time spent in the central area (B) and total distance (C) among groups in the OFT. Percentage of time spent immobile in the FST (D) and TST (E). * $p < 0.05$, ** $p < 0.01$, *** $p < 0.001$ vs. SI group, $n = 7$ /group.

[37,38]. Previous studies have shown that SI induces neuroinflammation and microglial overactivation [39]. This finding is consistent with our result that the expression of the microglial biomarker Iba1 in socially isolated mice was upregulated in the hippocampus, which is a brain region vulnerable to stress. We also found that SI led to depressive-like behavior in mice, which is consistent with previous studies [40,41]. Strikingly, SI increased locomotor activity compared with the GH group. Evidence has shown that chronic stress could enhance locomotor activity [42], which has the same result, although different stressors were used.

Microglia are resident macrophages of the central nervous system and play major roles in synaptic pruning, neurogenesis, neuroinflammation and endoplasmic reticulum stress in animal models of stress-induced depression [43,44]. Social isolation could give rise to depression behavior in rats induced by microglial activation [24]. There are many inhibitors of microglia, such as minocycline and clodronate [45,46], but studies have shown that they have different pharmacological effects. Minocycline, a tetracycline antibiotic, is able to cross the blood–brain barrier and exerts anti-inflammatory effects via microglial inhibition [47]. However, it is not a specific inhibitor of microglia and cannot delete microglia. As a member of the bisphosphonate family, clodronate administered to the brain can delete microglia, but it is potentially limited by the blood–brain barrier, astrocyte microanatomical domains, and the neurovascular network [48]. Inhibiting microglia with minocycline improved depression-like behavior induced by early-life social isolation in rats [24]. The specific role of microglia still needs further validation.

PLX3397, a selective CSF1R kinase inhibitor, is able to cross the blood–brain barrier and has a strong inhibitory effect on microglia [49]. Therefore, we used PLX3397 to delete microglia and observed its effects on the behavior of mice. We found that deleting microglia could alleviate depressive-like behavior, as indicated by the FST and TST. Evidence has shown that chronic stress induces microglial morphological remodeling to maintain homeostasis in the brain, such as amoeboid microglia with shorter and thicker processes, enlarged cell bodies, and fewer complex branches [50,51]. These results are in line with the microglial morphological changes induced by SI. PLX3397 1w could reverse the decrease in the length of microglial processes and the complexity caused by SI, which may be caused by repopulation after

drug withdrawal. Consistent with previous studies that microglial repopulation could promote an anti-inflammatory, and normalized proinflammatory gene expression [28]. However, we found that PLX3397 2w could not reverse the morphological changes of microglia because of the pharmacological effects of PLX3397.

Regulating synaptic plasticity, such as synapse maturation or elimination, is an important physiological function of microglia, which are involved in the pathological process of depression [52,53]. Previous studies have shown that neuroinflammation induced by microglia can modulate neuronal plasticity and neurogenesis [54,55]. Therefore, we evaluated the levels of inflammatory cytokines in the hippocampus. Our results demonstrated that PLX3397 treatment partially recovered the pro-/anti-inflammatory balance induced by microglial dysfunction, including the expression levels of the pro-inflammatory cytokines IL-1 β and iNOS and the anti-inflammatory cytokine Arg-1 [56]. In addition, we evaluated the protein levels of synaptic-associated protein and doublecortin (DCX) in the hippocampus by WB and observed the changes in dendrite length, number of dendrite branches and density of dendrite spines by Golgi staining. Our results indicated that PLX3397 treatment reversed the downregulation of DCX and GluR1 and restored the decrease in dendrite length and the reduced number of dendrite branches and density of dendrite spines caused by SI. Our results showed that PLX3397 treatment for one week had the same effect as PLX3397 treatment for two weeks, which was probably due to the protective role played by regenerated microglia [28]. Taken together, our results showed that PLX3397 could ameliorate depression-like behavior in mice, which was linked to maintaining the balance in pro-/anti-inflammatory cytokines, promoting neurogenesis, and enhancing synaptic plasticity.

In conclusion, our results showed that deleting microglia could alleviate depressive-like behavior in chronic socially isolated mice, which might be due to the rebalancing of pro-/anti-inflammatory cytokines, thus boosting neurogenesis and enhancing synaptic plasticity.

Ethics Statement

Ethics Committee approval was obtained from the Institutional Ethics Committee of Changsha Medical University to the commencement of the study. The approval numbers for ethical reviews is 20220509.

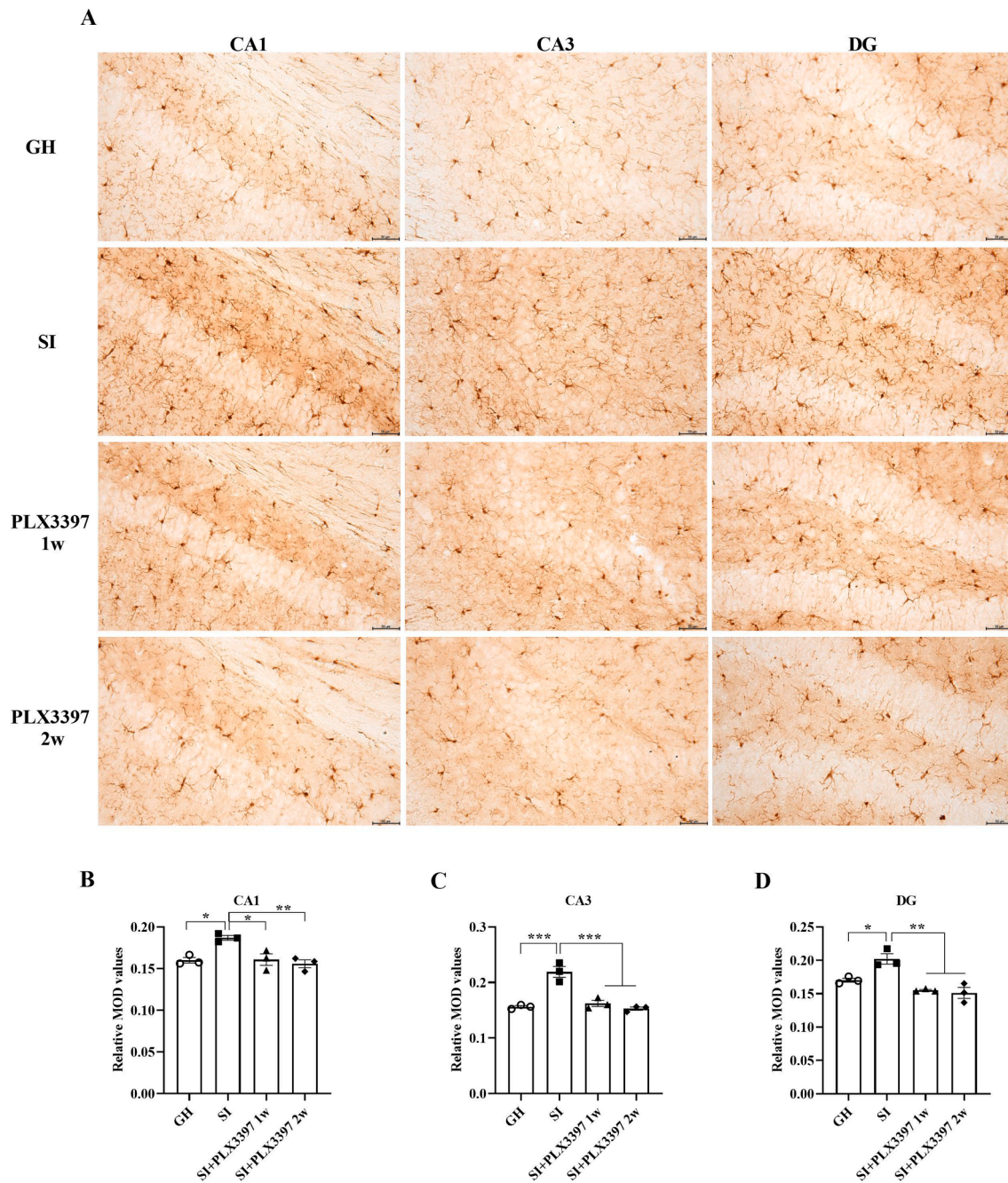


Fig. 4. PLX3397 treatment decreases the expression of Iba1 in the hippocampi of mice. (A) Representative image of Iba1 expression in the hippocampal CA1, CA3 and DG areas in four groups. The statistical results of Iba1 expression in the CA1 (B), CA3 (C) and DG (D) areas. * $p < 0.05$, ** $p < 0.01$, *** $p < 0.001$ vs. SI group, $n = 3$ /group, scale bar = 50 μm .

CRedit authorship contribution statement

Laifa Wang: . Xueqin Wang: . Ling Deng: . Hui Zhang: . Binsheng He: Resources. Wenyu Cao: Resources. Yanhui Cui: Resources.

Declaration of Competing Interest

The authors declare that they have no known competing financial

interests or personal relationships that could have appeared to influence the work reported in this paper.

Data availability

Data will be made available on request.

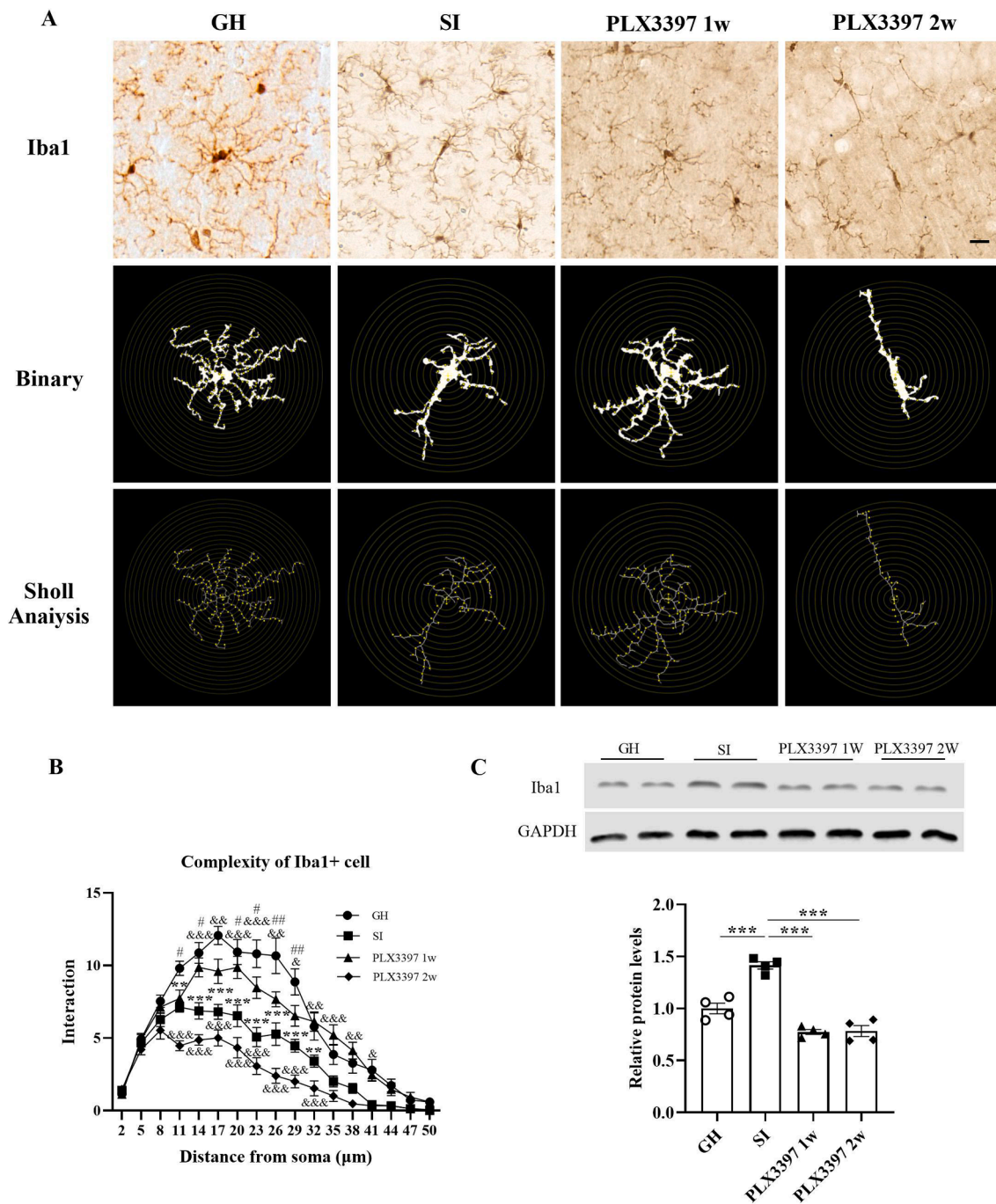


Fig. 5. Morphological changes of microglia in the hippocampus after PLX3397 treatment by Sholl analysis. (A) Representative images of Iba1⁺ cells are presented in the hippocampus in four groups. (B) Quantitative analyses of the complexity of Iba1⁺ cells. (C) Representative immunoblots and quantitative analyses of Iba1 expression in hippocampus. ***p* < 0.01, ****p* < 0.001 vs. SI group; &*p* < 0.05, &&*p* < 0.01, &&&*p* < 0.001 vs. PLX3397 1w group; #*p* < 0.05, ##*p* < 0.01 vs. PLX3397 2w group. *n* = 3/group, scale bar = 20 µm.

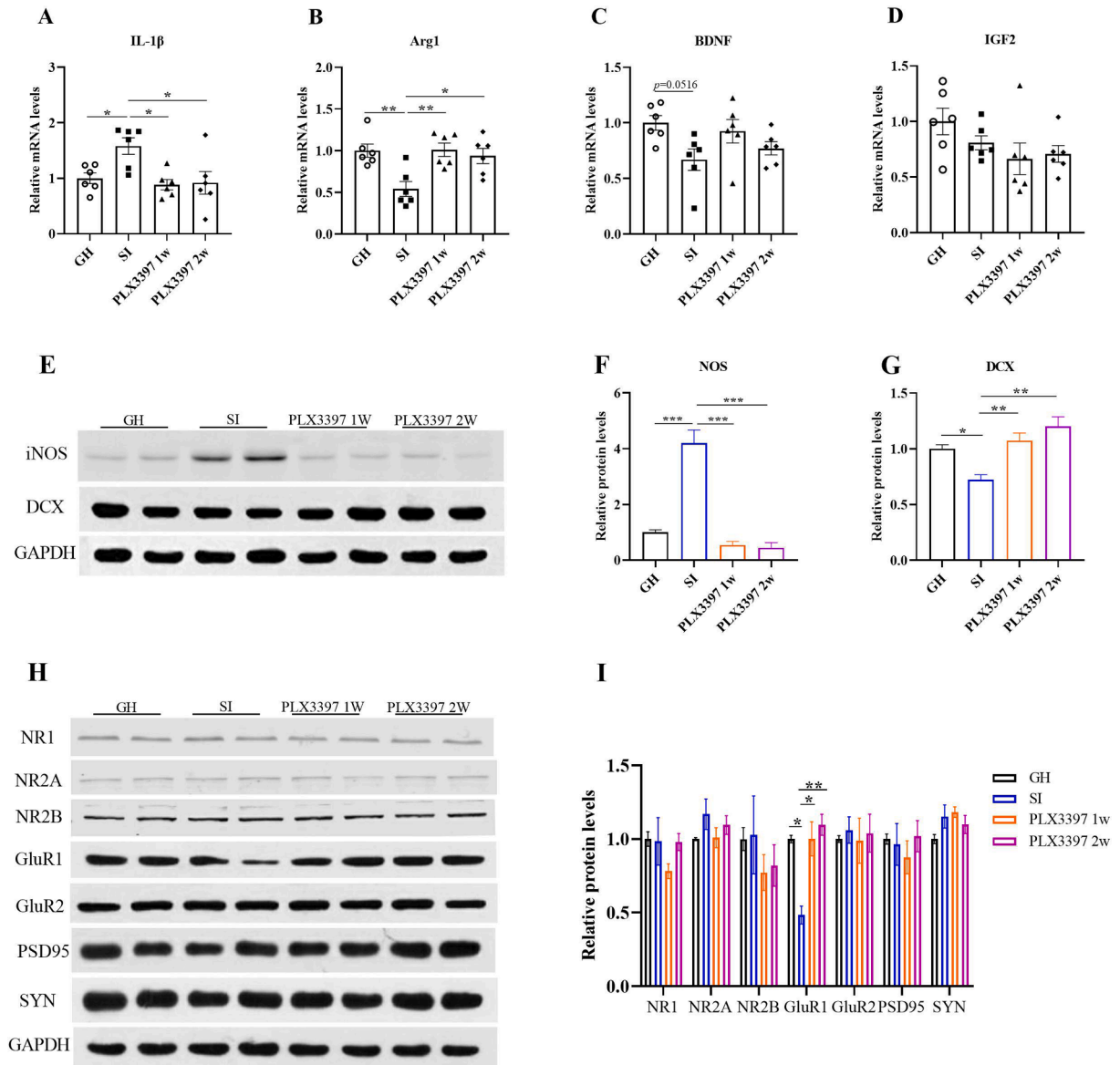


Fig. 6. Assessed inflammatory factors and synapse-associated proteins in different groups. (A-D) Changes in IL-1 β , Arg1, BDNF and IGF2 expression in the hippocampus, n = 6/group. (E-G) Representative bands and quantitative analyses of iNOS and DCX expression. (H-I) Representative images and quantitative analyses of NR1, NR2A, NR2B, GluR1, GluR2, PSD95 and SYN expression in different groups by WB. * $p < 0.05$, ** $p < 0.01$, *** $p < 0.001$ vs. SI group, n = 4/group.

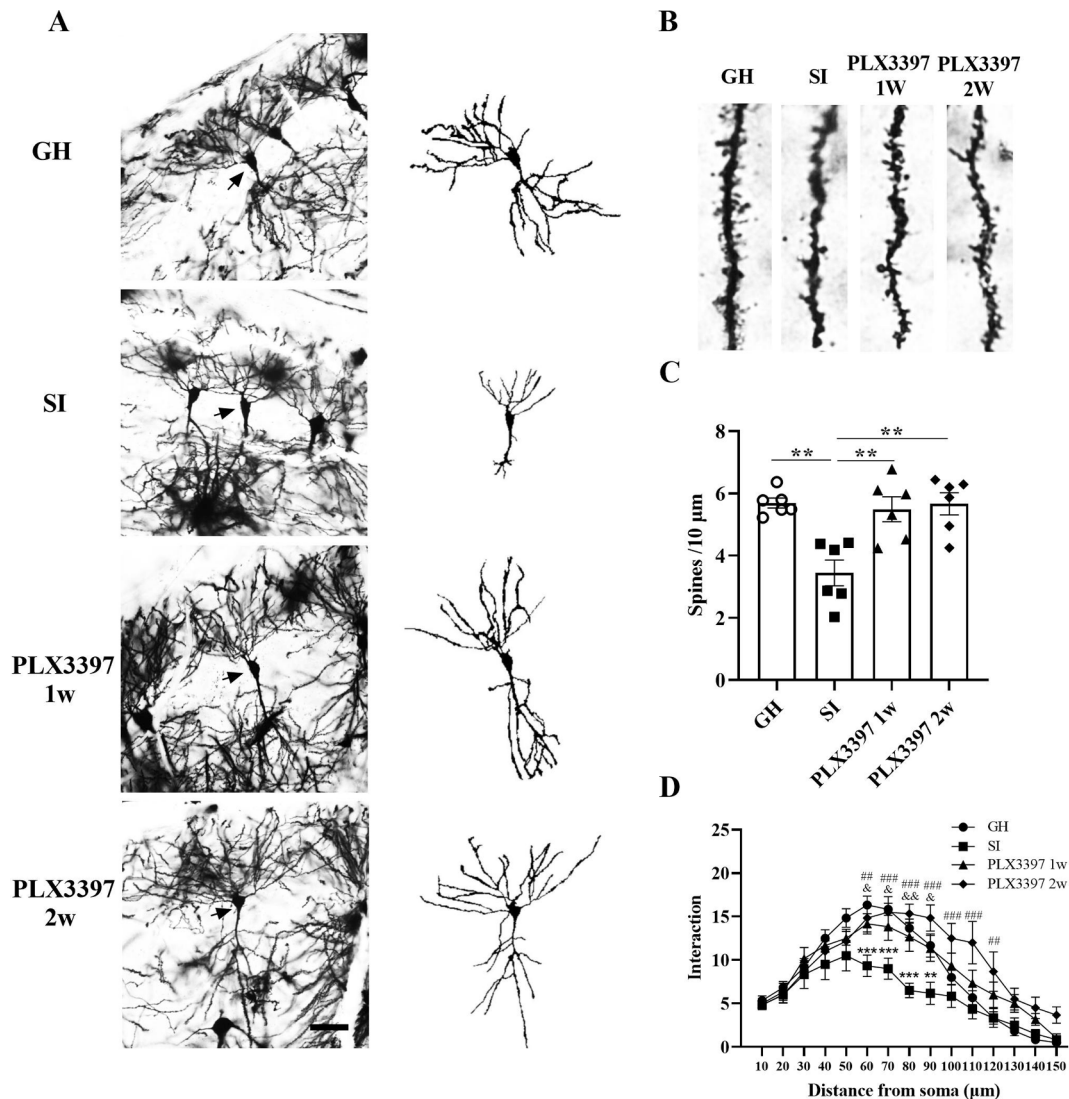


Fig. 7. Evaluation of the changes of neuronal branches and dendrite spine densities in the hippocampus by Golgi staining. (A) Images of Golgi staining and neuronal reconstruction in the hippocampi of mice. (B) Images of dendritic spines of neurons in the hippocampus. (C) Quantitative analyses of dendritic spine density after PLX3397 treatment. (D) Quantitative analyses of neuronal branches in the hippocampus by Sholl analysis. $^{**}p < 0.01$, $^{***}p < 0.001$ vs. SI group; $^{\#}p < 0.01$, $^{\#\#}p < 0.010$ vs. PLX3397 2w group; $^{\&}p < 0.05$, $^{\&\&}p < 0.01$ vs. PLX3397 1w group, $n = 3/\text{group}$, scale bar = 50 μm .

Acknowledgments

This work was supported by the Research Foundation of Education Bureau of Hunan Province, China (Program NO. 19B069, 19C0197 and 19C0220), the Natural Science Foundation of Changsha, China (kq2014117), the Natural Science Foundation of Hunan Province (Program No. 2020JJ5627), Hunan College Students Innovation and Entrepreneurship Training Program “The role of voltioxetine in post-traumatic stress disorder”.

References

- I. Zoicas, J. Kornhuber, The role of the N-methyl-D-aspartate receptors in social behavior in rodents[J], *Int. J. Mol. Sci.* 20 (22) (2019).
- L. Guo, L. An, F. Luo, et al., Social isolation, loneliness and functional disability in Chinese older women and men: a longitudinal study[J], *Age Ageing* 50 (4) (2021) 1222–1228.
- Y. Liu, J. Hu, J. Liu, Social support and depressive symptoms among adolescents during the COVID-19 pandemic: the mediating roles of loneliness and meaning in life[J], *Front. Public Health* 10 (2022), 916898.
- S. Lange, C.M. Altrrock, E. Gossmann, et al., COVID-19-what price do children pay? An analysis of economic and social policy factors[J], *Int. J. Environ. Res. Public Health* 19 (13) (2022).
- N. Pai, S.L. Vella, The physical and mental health consequences of social isolation and loneliness in the context of COVID-19[J], *Curr. Opin. Psychiatry* 35 (5) (2022) 305–310.
- R. Scendoni, P. Fedeli, M. Cingolani, The network of services for COVID-19 vaccination in persons with mental disorders: the Italian Social Health System, Its Organization, and Bioethical Issues[J], *Front. Public Health* 10 (2022), 870386.
- B. Yu, A. Steptoe, Y. Chen, et al., Social isolation, rather than loneliness, is associated with cognitive decline in older adults: the China Health and Retirement Longitudinal Study[J], *Psychol. Med.* 51 (14) (2021) 2414–2421.
- A. Freedman, J. Nicolle, Social isolation and loneliness: the new geriatric giants: approach for primary care[J], *Can. Fam. Physician* 66 (3) (2020) 176–182.
- A. Haj-Mirzaian, K. Ramezanzadeh, A. Tafazolimoghadam, et al., Protective effect of minocycline on LPS-induced mitochondrial dysfunction and decreased seizure threshold through nitric oxide pathway[J], *Eur. J. Pharmacol.* 858 (2019), 172446.
- A. Haj-Mirzaian, S. Amiri, H. Amini-Khoei, et al., Attenuation of oxidative and nitrosative stress in cortical area associates with antidepressant-like effects of tropisetron in male mice following social isolation stress[J], *Brain Res. Bull.* 124 (2016) 150–163.
- H. Mozafari, S. Amiri, S.E. Mehr, et al., Minocycline attenuates depressive-like behaviors in mice treated with the low dose of intracerebroventricular streptozotocin: the role of mitochondrial function and neuroinflammation[J], *Mol. Biol. Rep.* 47 (8) (2020) 6143–6153.
- A.S. Warden, S.A. Wolfe, S. Khom, et al., Microglia control escalation of drinking in alcohol-dependent mice: genomic and synaptic drivers[J], *Biol. Psychiatry* 88 (12) (2020) 910–921.
- X. Jia, Z. Gao, H. Hu, Microglia in depression: current perspectives[J], *Sci. China Life Sci.* 64 (6) (2021) 911–925.

- [14] A.P. Young, E.M. Denovan-Wright, Synthetic cannabinoids reduce the inflammatory activity of microglia and subsequently improve neuronal survival in vitro[J], *Brain Behav. Immun.* 105 (2022) 29–43.
- [15] E.C. Wright-Jin, D.H. Gutmann, Microglia as dynamic cellular mediators of brain function[J], *Trends Mol. Med.* 25 (11) (2019) 967–979.
- [16] D. Nayak, T.L. Roth, D.B. McGavern, Microglia development and function[J], *Annu. Rev. Immunol.* 32 (2014) 367–402.
- [17] E.N. Moca, D. Lecca, K.T. Hope, et al., Microglia drive pockets of neuroinflammation in middle age[J], *J. Neurosci.* 42 (19) (2022) 3896–3918.
- [18] C. Madore, Z. Yin, J. Leibowitz, et al., Microglia, lifestyle stress, and neurodegeneration[J], *Immunity* 52 (2) (2020) 222–240.
- [19] D.D. Tian, M. Wang, A. Liu, et al., Antidepressant effect of paeoniflorin is through inhibiting pyroptosis CASP-11/GSDMD pathway[J], *Mol. Neurobiol.* 58 (2) (2021) 761–776.
- [20] C. Fan, Y. Li, T. Lan, et al., Microglia secrete miR-146a-5p-containing exosomes to regulate neurogenesis in depression[J], *Mol. Ther.* 30 (3) (2022) 1300–1314.
- [21] B. Bassett, S. Subramaniam, Y. Fan, et al., Minocycline alleviates depression-like symptoms by rescuing decrease in neurogenesis in dorsal hippocampus via blocking microglia activation/phagocytosis[J], *Brain Behav. Immun.* 91 (2021) 519–530.
- [22] B. Wang, X. Huang, X. Pan, et al., Minocycline prevents the depressive-like behavior through inhibiting the release of HMGB1 from microglia and neurons[J], *Brain. Behav. Immun.* 88 (2020) 132–143.
- [23] Y. Gong, L. Tong, R. Yang, et al., Dynamic changes in hippocampal microglia contribute to depressive-like behavior induced by early social isolation[J], *Neuropharmacology* 135 (2018) 223–233.
- [24] H.T. Wang, F.L. Huang, Z.L. Hu, et al., Early-life social isolation-induced depressive-like behavior in rats results in microglial activation and neuronal histone methylation that are mitigated by minocycline[J], *Neurotox Res* 31 (4) (2017) 505–520.
- [25] M. Orylska-Ratynska, W. Placek, A. Owczarczyk-Saczonek, Tetracyclines – an important therapeutic tool for dermatologists[J], *Int. J. Environ. Res. Public Health* 19 (12) (2022).
- [26] L. Yang, J. Yang, H. Liu, et al., Minocycline binds and inhibits LYN activity to prevent STAT3-mediated metastasis of colorectal cancer[J], *Int. J. Biol. Sci.* 18 (6) (2022) 2540–2552.
- [27] M.R. Elmore, A.R. Najafi, M.A. Koike, et al., Colony-stimulating factor 1 receptor signaling is necessary for microglia viability, unmasking a microglia progenitor cell in the adult brain[J], *Neuron* 82 (2) (2014) 380–397.
- [28] L.J. Coleman, J. Zou, F.T. Crews, Microglial depletion and repopulation in brain slice culture normalizes sensitized proinflammatory signaling[J], *J. Neuroinflammation.* 17 (1) (2020) 27.
- [29] L. Ren, H. Zhang, W. Tao, et al., The rapid and long-lasting antidepressant effects of iridoid fraction in gardenia *Jasminoides* J. Ellis Are Dependent on Activating PKA-CREB Signaling Pathway[J], *Front Pharmacol.* 2022,13:896628.
- [30] Y.H. Cui, A. Fu, X.Q. Wang, et al., Hippocampal LASP1 ameliorates chronic stress-mediated behavioral responses in a mouse model of unpredictable chronic mild stress[J], *Neuropharmacology* 184 (2021), 108410.
- [31] Z.D. Kabir, A.S. Lee, C.E. Burgdorf, et al., Cacna1c in the prefrontal cortex regulates depression-related behaviors via REDD1[J], *Neuropsychopharmacology* 42 (10) (2017) 2032–2042.
- [32] S.J. Li, L.X. Zhang, G.J. Zou, et al., Infralimbic YTHDF1 is necessary for the beneficial effects of acute mild exercise on auditory fear extinction retention[J], *Cereb Cortex* (2022).
- [33] F. Zhong, L. Liu, J.L. Wei, et al., Step by step golgi-cox staining for cryosection[J], *Front Neuroanat* 13 (2019) 62.
- [34] L. Niu, S.S. Luo, Y. Xu, et al., The critical role of the hippocampal NLRP3 inflammasome in social isolation-induced cognitive impairment in male mice[J], *Neurobiol. Learn Mem.* 175 (2020), 107301.
- [35] Y. Yang, Z.H. Wang, S. Jin, et al., Opposite monosynaptic scaling of BLP-vCA1 inputs governs hopefulness- and helplessness-modulated spatial learning and memory[J], *Nat. Commun.* 7 (2016) 11935.
- [36] K. Young, H. Morrison, Quantifying microglia morphology from photomicrographs of immunohistochemistry prepared tissue using ImageJ[J], *J. Vis. Exp.* 136 (2018).
- [37] F. Mumtaz, M.I. Khan, M. Zubair, et al., Neurobiology and consequences of social isolation stress in animal model-A comprehensive review[J], *Biomed. Pharmacother.* 105 (2018) 1205–1222.
- [38] J.T. Cacioppo, S. Cacioppo, J.P. Capitanio, et al., The neuroendocrinology of social isolation[J], *Annu. Rev. Psychol.* 66 (2015) 733–767.
- [39] N.C. Ferrara, S. Trask, L. Yan, et al., Isolation driven changes in Iba1-positive microglial morphology are associated with social recognition memory in adults and adolescents[J], *Neurobiol. Learn. Mem.* 192 (2022), 107626.
- [40] Y.D. Gilles, E.K. Polston, Effects of social deprivation on social and depressive-like behaviors and the numbers of oxytocin expressing neurons in rats[J], *Behav. Brain Res.* 328 (2017) 28–38.
- [41] W. Li, L. Niu, Z. Liu, et al., Inhibition of the NLRP3 inflammasome with MCC950 prevents chronic social isolation-induced depression-like behavior in male mice[J], *Neurosci. Lett* 765 (2021), 136290.
- [42] L.F. Li, J. Yang, S.P. Ma, et al., Magnolol treatment reversed the glial pathology in an unpredictable chronic mild stress-induced rat model of depression[J], *Eur. J. Pharmacol.* 711 (1–3) (2013) 42–49.
- [43] N. Rimmerman, H. Verdiger, H. Goldenberg, et al., Microglia and their LAG3 checkpoint underlie the antidepressant and neurogenesis-enhancing effects of electroconvulsive stimulation[J], *Mol. Psychiatry* 27 (2) (2022) 1120–1135.
- [44] X. Xu, H.N. Piao, F. Aosai, et al., Arctigenin protects against depression by inhibiting microglial activation and neuroinflammation via HMGB1/TLR4/NF-kappaB and TNF-alpha/TNFR1/NF-kappaB pathways[J], *Br. J. Pharmacol.* 177 (22) (2020) 5224–5245.
- [45] C.M. Sellgren, J. Gracias, B. Watmuff, et al., Increased synapse elimination by microglia in schizophrenia patient-derived models of synaptic pruning[J], *Nat. Neurosci.* 22 (3) (2019) 374–385.
- [46] X. Han, Q. Li, X. Lan, et al., Microglial depletion with clodronate liposomes increases proinflammatory cytokine levels, induces astrocyte activation, and damages blood vessel integrity[J], *Mol. Neurobiol.* 56 (9) (2019) 6184–6196.
- [47] C.R. Coker, M. White, A. Singal, et al., Minocycline reduces hypothalamic microglia activation and improves metabolic dysfunction in high fat diet-induced obese mice[J], *Front Physiol.* 13 (2022), 933706.
- [48] E. McCloskey, A.H. Paterson, T. Powles, et al., Clodronate[J], *Bone* 143 (2021), 115715.
- [49] D.E. Marzan, V. Brugger-Verdon, B.L. West, et al., Activated microglia drive demyelination via CSF1R signaling[J], *Glia* 69 (6) (2021) 1583–1604.
- [50] M. Gold, A.M. Dolga, J. Koepke, et al., alpha1-antitrypsin modulates microglial-mediated neuroinflammation and protects microglial cells from amyloid-beta-induced toxicity[J], *J. Neuroinflammation* 11 (2014) 165.
- [51] R. Yirmiya, N. Rimmerman, R. Reshef, Depression as a microglial disease[J], *Trends Neurosci.* 38 (10) (2015) 637–658.
- [52] R.S. Duman, G.K. Aghajanian, G. Sanacora, et al., Synaptic plasticity and depression: new insights from stress and rapid-acting antidepressants[J], *Nat. Med.* 22 (3) (2016) 238–249.
- [53] B. Xu, Q. Li, Y. Wu, et al., Mettl3-mediated m(6) A modification of Lrp2 facilitates neurogenesis through Ythdc2 and elicits antidepressant-like effects[J], *FASEB J.* 36 (7) (2022) e22392.
- [54] Z.H. Zheng, J.L. Tu, X.H. Li, et al., Neuroinflammation induces anxiety- and depressive-like behavior by modulating neuronal plasticity in the basolateral amygdala[J], *Brain Behav. Immun.* 91 (2021) 505–518.
- [55] K.G. Witcher, C.E. Bray, T. Chunchai, et al., Traumatic brain injury causes chronic cortical inflammation and neuronal dysfunction mediated by microglia[J], *J. Neurosci.* 41 (7) (2021) 1597–1616.
- [56] S. Li, W. Cao, S. Zhou, et al., Expression of Cntn1 is regulated by stress and associated with anxiety and depression phenotypes[J], *Brain Behav. Immun.* 95 (2021) 142–153.